



ELSEVIER

Journal of Nuclear Materials 275 (1999) 158–163

Journal of
nuclear
materials

www.elsevier.nl/locate/jnucmat

Nitrogen implantation into carbon: retention, release and target-erosion processes

S. Grigull^{a,b,*}, R. Behrisch^a, S. Parascandola^b

^a Max-Planck-Institut für Plasmaphysik, Euratom Association, 85748 Garching, Germany

^b Forschungszentrum Rossendorf, Institut für Ionenstrahlphysik und Materialforschung, 01314 Dresden, Germany

Received 8 February 1999; accepted 8 April 1999

Abstract

The interaction of nitrogen ions with carbon films is investigated in view of the nitrogen recycling behavior on carbon divertor targets during plasma operation with nitrogen gas puffing. Nitrogen ion implantation is carried out in the energy range between 0.75 and 20 keV and at irradiation temperatures between room temperature and 800°C. Nitrogen retention and release are analyzed in situ, using elastic recoil detection and time-resolved residual gas analysis, respectively. It is found that the nitrogen contents inside the implanted near-surface layers saturate at large fluences, and that the temperature and energy dependence of the saturation level is qualitatively different from the behavior found for the bombardment of graphite surfaces with hydrogen ions. The different behavior is mainly attributed to the formation of N₂ bubbles in the implanted near-surface layers. The N₂ formation is also identified as the driving force for nitrogen saturation and release at large fluences. It is concluded that nitrogen interacting with carbon surfaces cannot be regarded as a non-recycling gas under high-dosage irradiation conditions. © 1999 Published by Elsevier Science B.V. All rights reserved.

1. Introduction

In divertor tokamak experiments, nitrogen gas injection is used during the discharges to achieve a controlled radiative cooling of the divertor boundary layer and a detached state of the divertor plasma with strongly reduced energy fluxes onto the target [1,2]. In the case of short discharges lasting a few seconds, it was found that nitrogen is gettered by the carbon walls, with the result that it is considered as a non-recycling gas [3]. However, this may not be valid for long-lasting discharges where the near-surface layers of the walls become saturated with nitrogen, and the nitrogen recycling coefficient is close to one. It is the topic of the present work to investigate the nitrogen retention and release behavior of carbon surfaces during irradiation with energetic N ions.

In the past, ion-beam irradiation studies have made a significant contribution to understanding the interaction of high-temperature hydrogen plasmas with graphite surfaces [4,5]. Compared to the irradiation with plasmas [6], the use of mass-separated and monoenergetic ion beams offers the advantage of a sufficient control over the dependence of the retention and release behavior of the implanted species on individual irradiation parameters, such as particle mass, flux and energy, respectively. In this work, ion-beam studies are presented on the dependence of the nitrogen retention on irradiation fluence, temperature and energy. Retention data were obtained using a dual ion-beam setup with a keV ion implanter for N ion irradiation and a MeV heavy-ion beam for in situ compositional analysis of the irradiated material via the elastic recoil detection analysis (ERDA) technique [7,8]. While most of the measurements were carried out at a fixed implantation energy of 20 keV and on diamond-like carbon (ta-C) films, it is also discussed to what extent the nitrogen retention may be different if lower irradiation energies or other carbonic materials are used. The nitrogen release during bombardment was

* Corresponding author. Present address: ESRF, BP 220, F-38043 Grenoble cedex, France. Tel.: +33-4 76 88 24 47; fax: +33-4 76 88 27 07; e-mail: grigull@esfr.fr

investigated using residual gas analysis (RGA). Target erosion rates are given for different irradiation conditions. A brief discussion addresses possible implications for nitrogen-puffed divertor plasmas.

2. Experiment

Thin films of ta-C of typically 250 nm thickness were prepared by the filtered cathodic arc technique on sputter-cleaned Si substrates [9]. Although the material relevant for fusion devices is graphite, ta-C thin films were used for the following reasons:

1. Compared to graphite, the films display smooth surfaces which are mandatory for ion-beam analyses techniques using glancing angles, such as ERDA [10].
2. The finite thickness of the layers allows an easy measurement of the target erosion rates by analyzing the changes in the total carbon areal densities.
3. In low-density carbon materials such as graphite, nitrogen bulk diffusion was observed for irradiation at elevated temperatures [11,12], while the diamond-like atomic structure of ta-C, with a high density of 3.0 g/cm³, ensures confinement of the nitrogen inventory within the implanted subsurface region. This is important for studies of the saturation and release mechanism at large irradiation fluences [13].

Ion-beam irradiation and analysis were carried out in the Rossendorf dual ion-beam facility [13]. Mass analyzed N⁺ ions of typically 20 keV were used for the irradiation at ion fluxes of about 1×10^{14} cm²/s. This energy is much higher than typical particle energies in divertor plasmas, but generates ion penetration depths sufficiently large compared to the depth resolution achievable with the analyzing 35 MeV Cl⁷⁺ ion beam of 5–7 nm, to obtain reasonably analyzable nitrogen depth profiles. In few cases where N ions were used at lower energies, this is mentioned in the text. The two beams were operated at angles of 6.5° (N⁺) and 83.5° (Cl⁷⁺) relative to the surface normal of the carbon targets. The flux associated with the MeV analyzing beam was about 1×10^{11} cm²/s.

Time-resolved RGA measurements were carried out during N⁺ implantation using a quadrupole mass spectrometer. To discriminate nitrogen re-emitted from the target surface from signals originating from residual-gas nitrogen, the implanter was operated with ¹⁵N₂ gas. The RGA analyses were carried out separately from the dual-beam measurements. Target erosion studies were made at different temperatures using a Kaufmann ion gun operating at 1.5 keV and about 5×10^{14} ions cm²/s, with N₂⁺ as the predominating species in the irradiating beam. After irradiation, the residual carbon-film thickness of the respective samples were analyzed *ex situ* using Rutherford backscattering spectrometry (RBS).

3. Results

The nitrogen inventory buildup inside the carbon films during implantation at room temperature (RT) and 400°C is shown in Fig. 1. Total nitrogen contents were obtained by integrating the depth profiles measured while operating the MeV analyzing beam simultaneously with the implanting 20 keV N⁺ ion beam. At RT, the nitrogen content shows a saturation behavior similar to that found for hydrogen or helium implantation into graphite [5,14], with a linear increase and 100% retention at small fluences ($<1.5 \times 10^{17}$ N⁺/cm²) and 100% re-emission at large fluences ($>3 \times 10^{17}$ N⁺/cm²). The ERDA probing depth is larger than the C film thickness of 240 nm, compared to a thickness of the implanted sublayer of about 45 nm, so that nitrogen diffusion into the bulk can be ruled out.

Implantation at 400°C leads to nitrogen saturation at a smaller fluence, compared to RT. At 1.6×10^{17} N⁺/cm², an ‘overshoot’ 10–15% of the nitrogen content is observed with respect to the saturation level, which is not present at RT. Depth resolved analysis shows that at this fluence, the local nitrogen concentration in the depth region near the implantation maximum (20–30 nm) is 80% higher than in the saturated case, and close to the maximum RT nitrogen concentration at saturation corresponding to a nitrogen-to-carbon ratio of [N]/[C]=0.35. At both temperatures, the nitrogen contents remained constant when the implanting beam was turned off, indicating that no ‘dynamic’ component exists in the inventory.

Nitrogen saturation is determined by a maximum local [N]/[C] ratio inside the implanted depth range. This is concluded from the observation that the maximum

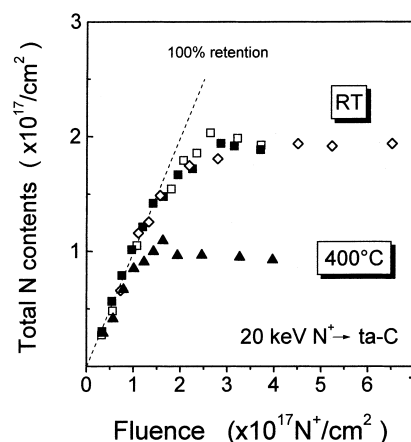


Fig. 1. Total nitrogen contents vs. N⁺ fluence during irradiation at room temperature and 400°C. Different symbols represent different samples.

concentration (saturation level) seems not to vary over a wide range of irradiation energies (see below). However, the $[N]/[C]$ saturation level shows a characteristic dependence on irradiation temperature. For 20 keV N^+ bombardment of ta-C, a comparatively sharp drop of more than 50% of the saturation level is observed at about 150°C, with only a weak temperature dependence for $T > 200^\circ\text{C}$ (Fig. 2). A similar curve is obtained for the total nitrogen contents. Low temperature implantation data into graphite [12] indicate that only slightly higher nitrogen concentrations are achieved at temperatures below RT (dashed line in Fig. 2).

The ‘discontinuous’ temperature characteristics with a ‘‘transition temperature’’ T_c of 150°C is indicative of a structural phase transformation inside the implanted N:C sub-layer of the films. In recent work, it was shown that the higher saturation level below T_c is correlated with the formation of N_2 gas bubbles during N irradiation which serve as an additional nitrogen reservoir inside the films, while these bubbles were not observed at 400°C [15]. It was found that about 50% of the nitrogen inventory at saturation consists of bubble N_2 , and can be thermally desorbed at 900°C. The remaining part formed covalent bonds with the C matrix, and proved to be thermally stable at this temperature [15,13].

The temperature dependence of the nitrogen concentration at saturation as measured for 20 keV N^+ irradiation of glassy carbon is different from the ta-C curve only above 200°C (Fig. 2). The stronger decrease of the nitrogen concentration at elevated temperatures, compared to ta-C, is attributed to nitrogen diffusion into

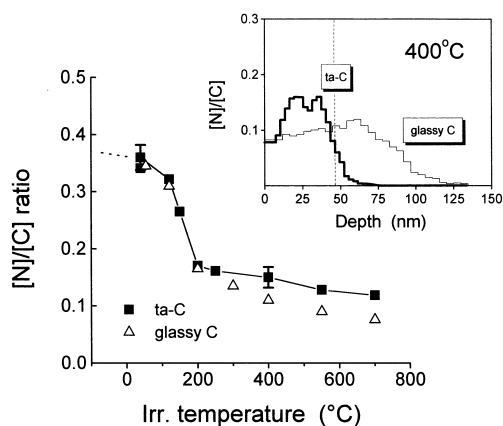


Fig. 2. Temperature dependence of the maximum local nitrogen concentration at saturation for 20 keV N^+ implantation into ta-C and glassy C, respectively. The inset shows saturated nitrogen depth profiles obtained at 400°C after irradiation with a fluence of $4 \times 10^{17} N^+/\text{cm}^2$ in the two different materials. The depth scales of the two profiles are normalized to an identical C density of 3.0 g/cm^3 .

the depth region adjacent to the implanted sub-layer (see depth profiles, inset Fig. 2), which has a low density of 1.4 g/cm^3 . In ta-C films which have a very high density of 3.0 g/cm^3 , the unimplanted depth region acts as a nitrogen diffusion barrier. Structural analyses in recent work have shown that the implanted sub-layer in ta-C transforms into a material with graphitic properties, at a density of about 1.7 g/cm^3 for implantation at both RT and 400°C [13].

The RT saturation level of $[N]/[C]=0.35$ does not significantly depend on the irradiation energy in the range 4–50 keV. This is inferred from the depth profiles given in Fig. 3 and from data available from existing work on nitrogen implantation into glassy C, graphite and diamond films, respectively [16–18]. It is assumed that in this energy range the RT saturation level is identical for the three different carbon modifications, which is supported by the ta-C and glassy C data in Fig. 2 and studies in Refs. [17,18]. However, at an irradiation energy of 3 keV, the present authors found a drop of the maximum nitrogen concentration at saturation by about 50%, compared to 4 keV (see Fig. 3). This is an indication that different physical processes determine the nitrogen retention and release behavior at lower energies.

From transmission electron microscopy analyses [15], the authors assume that the N^+ ion range at 4 keV is comparable to the minimum dimension of stable N_2 bubbles which may not form at even smaller energies, leading to smaller nitrogen saturation levels below this ‘‘threshold’’ energy. Another different nitrogen retention and release scenario seems to be present at even lower irradiation energies and elevated temperatures: A ta-C film implanted at 400°C with 1.5 keV N_2^+ ions, using the

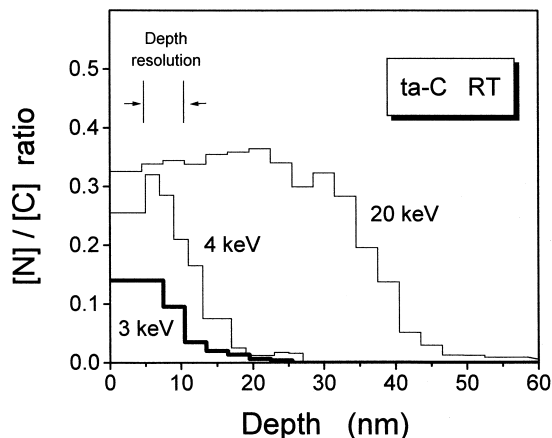


Fig. 3. Saturated nitrogen depth profiles for different N^+ irradiation energies at RT. The respective fluences are $4 \times 10^{17} N^+/\text{cm}^2$ (20 keV), $0.7 \times 10^{17} N^+/\text{cm}^2$ (4 keV) and $0.3 \times 10^{17} N^+/\text{cm}^2$ (3 keV).

Kaufmann ion source, showed a maximum $[N]/[C]$ ratio of 0.4. This is almost three times as much as obtained at 20 keV (see Fig. 2).

The nitrogen saturation and release at RT and large irradiation fluences are governed by the formation of N_2 molecules inside the implanted sub-layer and their subsequent migration to and re-emission from the surface, respectively. This was concluded from RGA measurements during 20 keV N^+ implantation into ta-C [13]. Fig. 4 shows the evolution in time of three different nitrogen-related mass signals during $^{15}N^+$ irradiation. Differently from the mass-28 signal (M28) and from M14, M18 and M29 (not shown), the M30 signal has a characteristic time dependence which is anti-correlated to that of the nitrogen inventory of the implanted films: An increase from the background level of 5×10^{-8} mbar after about 5 min implantation time, corresponding to a fluence of $1 \times 10^{17} N^+/cm^2$, is followed by saturation on a significantly higher level after another 10 min of irradiation. The same behavior is observed after shifting the beam to an unexposed target region, as shown in the figure.

Additional experiments have demonstrated that the rise in the M30 signal corresponds indeed to the re-emission of N_2 from the irradiated samples, and that the implanted N atoms recombine to N_2 molecules inside

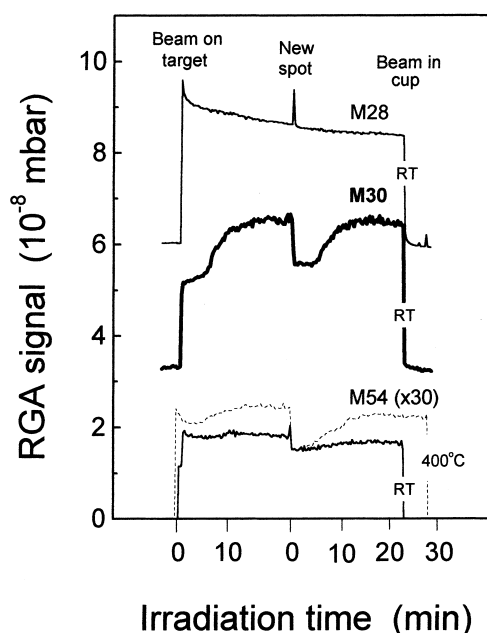


Fig. 4. RGA trends for different N-related masses recorded during irradiation of ta-C with 20 keV N^+ ions at RT and 400°C resp. 4.8 min irradiation time correspond to $1 \times 10^{17} N^+/cm^2$. The M30 signal represents the absolute partial pressure of this mass while the other trends are vertically shifted for clarity.

the implanted sub-layer and not at the surface of the films [13]. This behavior is comparable with observations made for hydrogen irradiation of graphite [5,19], and fits qualitatively with the Local Saturation Model developed by Möller et al. [20]. In the case of N^+ irradiation at 400°C, indications for the re-emission of atomic nitrogen have been found [13], similar to observations made by Franzen et al. during hydrogen bombardment of graphite at elevated temperatures [21]. Also, a significant re-emission signal is observed on mass 54, compared to RT irradiation (see Fig. 4) which is an indication of a ‘chemical’ erosion of the films through the formation of volatile C_2N_2 at elevated temperatures (see Ref. [22]).

Measurements of the N^+ sputtering yield at 20 keV did not show a significant temperature dependence in the range between RT and 700°C, which is consistent with the relatively weak M54 re-emission signal in Fig. 4, compared to M30. Obviously, the ‘chemical’ component of the target erosion is negligibly small at this energy, compared to the physical sputtering yield of 0.25 C atoms per incident N^+ ion [13]. At lower irradiation energies, the formation of C_2N_2 would be confined to smaller depths, and chemical effects should be more important for the target erosion than at 20 keV.

Irradiation experiments on ta-C films using fluences of about $2 \times 10^{18}/cm^2$ of 1.5 keV N_2^+ ions showed indeed a significant increase of the sputtering yield at elevated temperatures. Fig. 5 shows data obtained from RBS analyses of the C-film thickness before and after irradiation at different temperatures. Between 180°C and 800°C, the sputtering yield increases from 0.54 to 0.75°C atoms per incoming N atom, assuming that N_2^+ accounts for 100% of the species emitted from the ion source. The temperature dependence is indicative of a chemical

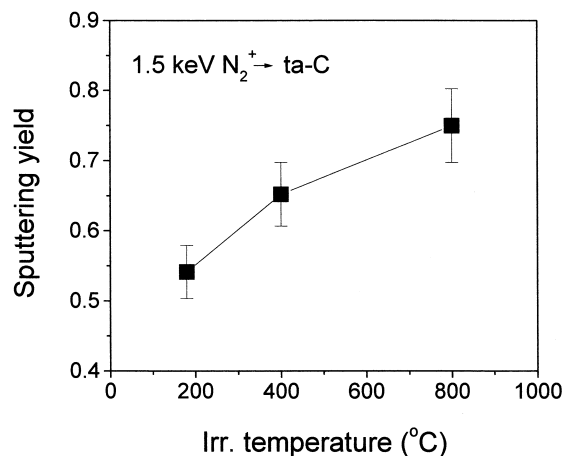


Fig. 5. Sputtering yield for irradiation of ta-C with 1.5 keV N_2^+ ions at three different temperatures.

component in the sputtering process. Such effects have been found and extensively studied in hydrogen irradiation experiments on graphite [23,24].

4. Discussion

The results in Fig. 1 show that at large irradiation fluences of about 10^{17} N⁺/cm² on carbon surfaces, the implanted near-surface layers get saturated with nitrogen, and 100% of the implanted atoms are re-emitted into the vacuum. At energies below 20 keV, the threshold fluence for re-emission will be lower since the saturation is a local effect, and nitrogen penetration depths are smaller. As a result, when injected into a divertor with carbon targets during plasma discharges, nitrogen cannot be regarded as a non-recycling gas at large exposure times. Although downstream transport may lead to a recycling factor < 1 in low-density carbon at typical divertor operation temperatures, it is unlikely that the recycling will be small enough to control the nitrogen content in the plasma by the N₂ injection rate.

Since it was found that a high percentage of the retained nitrogen cannot be thermally desorbed at least up to 900°C [13,15] sputtering seems to be the most efficient method to get rid of unwanted nitrogen inventories that build up in the near-surface layer of the divertor target during plasma operation.

If N₂ bubble formation occurs under the more complex irradiation conditions in the plasma boundary layer, i.e. broad energy and angular distributions of the bombarding species, as it was observed for a 20 keV ion-beam at RT and normal incidence, this could result in irregular re-emission processes (spikes), which were found during He-ion bombardment of graphite [25]. However, since bubbles were only observed within a layer very close to the surface, and seem not to form at irradiation energies < 4 keV (see discussion Fig. 3), it is expected that the continuous co-bombardment of the target surface with high fluxes of low-energy nitrogen and hydrogen will inhibit the formation of the bubbles through high-rate sputtering.

As a consequence of the discussion of Fig. 3, it is obvious that the experimental data given in the present work cannot directly be extrapolated to the irradiation conditions in a nitrogen-puffed divertor plasma, where the mean particle energies are in the range of 50 eV and broad distributions of both irradiation energy and direction exist, plus a high-flux co-irradiation of hydrogen ions and neutrals. It is therefore desirable to perform quantitative analyses of the nitrogen depth distribution in carbon samples that have been exposed to nitrogen-puffed single-run divertor plasmas at different discharge lengths. As a second route, nitrogen ion irradiation experiments should be performed at very low energies, and possibly with alternating eV and keV exposure, to find

out if N₂ bubble formation is a relevant problem under conditions closer to divertor plasma scenarios.

5. Conclusions

The nitrogen retention and release behavior of diamond-like carbon films during irradiation with energetic N ions have been studied in situ. It is found that the nitrogen content inside the films saturates at large irradiation fluences on a concentration level that depends on both irradiation temperature and energy. At room temperature and a N⁺ ion energy of 20 keV, nitrogen re-emission sets in at a fluence of 1.5×10^{17} N⁺/cm² and reaches 100% when the nitrogen content inside the carbon layer is saturated at 2×10^{17} /cm². For irradiation at temperatures in the range of 200–700°C, a reduction of the saturated nitrogen contents by more than 50% is found compared to RT. Under RT irradiation, N₂ bubbles form in the implanted layer and lead to an increase of the nitrogen retention. No spontaneous release of nitrogen is observed at any temperature when the implanting beam is turned-off.

With increasing temperature, thermally activated transport of nitrogen towards the bulk is observed in low-density glassy carbon, an effect also reported for graphite in previous work.

While the maximum RT nitrogen-to-carbon ratio at saturation seems to be constant at about 0.35 for irradiation energies between 4 and 50 keV, a significantly smaller level is found at 3 keV, indicating that the 20 keV results cannot be extrapolated to very low energies.

The predominating nitrogen release pathway during high-fluence irradiation with 20 keV N⁺ is the formation and re-emission of N₂. At elevated temperatures, indications are found of the formation of volatile C₂N₂. High-fluence irradiation of the films with 1.5 keV N₂⁺ ions at temperatures between 180°C and 800°C result in temperature dependent sputtering yields, giving further confirmation for the existence of a chemical erosion related to the formation of C₂N₂.

Further systematic irradiation studies at lower ion energies and compositional analyses of plasma exposed divertor–target segments are necessary to obtain quantitative predictions for the nitrogen recycling behavior in tokamak experiments.

References

- [1] B. Lipschultz, J. Goetz, B. LaBombard et al., *J. Nucl. Mater.* 220–222 (1995) 50.
- [2] G.F. Matthews, *J. Nucl. Mater.* 220–222 (1995) 104.
- [3] B. Lipschultz, J.A. Goetz, B. LaBombard, G.M. McCracken, H. Ohkawa, Y. Takase, J.L. Terry, *J. Nucl. Mater.* 241–243 (1997) 771.

- [4] R.A. Langley, R.S. Blewer, J. Roth, *J. Nucl. Mater.* 76&77 (1978) 313.
- [5] W. Möller, P. Børgesen, B.M.U. Scherzer, *Nucl. Instrum. and Meth. B* 19 20 (1987) 826.
- [6] M. Langhoff, B.M.U. Scherzer, *J. Nucl. Mater.* 245 (1997) 60.
- [7] J. L'Ecuyer, J.A. Davies, N. Matsunami, *Nucl. Instrum. and Meth.* 160 (1979) 337.
- [8] U. Kreissig, R. Grötzschel, R. Behrisch, *Nucl. Instrum. and Meth. B* 85 (1994) 71.
- [9] M. Kühn, P. Meja, F. Richter, *Diamond Relat. Mater.* 2 (1993) 1350.
- [10] R. Behrisch, S. Grigull, U. Kreissig, R. Groetzschel, *Nucl. Instrum. and Meth. B* 136–138 (1998) 628.
- [11] A. Hoffman, I. Gouzman, R. Brener, *Appl. Phys. Lett.* 64 (1994) 845.
- [12] J. Hartmann, A. Königer, H. Huber, W. Ensinger, W. Assmann, B. Stritzker, B. Rauschenbach, *Nucl. Instrum. and Meth. B* 117 (1996) 392.
- [13] S. Grigull, W. Jacob, D. Henke, C. Spaeth, L. Suemmchen, W. Sigle, *J. Appl. Phys.* 83 (1998) 5185.
- [14] G. Ramos, B.M.U. Scherzer, *Nucl. Instrum. and Meth. B* 85 (1994) 479.
- [15] S. Grigull, W. Jacob, D. Henke, A. Mücklich, C. Spaeth, L. Sümchen, *Appl. Phys. Lett.* 70 (1997) 1387.
- [16] A. Hoffmann, H. Geller, I. Gouzman, C. Cytermann, R. Brener, M. Kenny, *Surf. Coat. Technol.* 68&69 (1994) 616.
- [17] A. Hoffman, M.J. Kenny, L.S. Wielunski, C. Cyterman, R. Brener, R.A. Clissold, in: *Proceedings of the Ninth International Conference on Ion Beam Modification of Materials*, Canberra, Australia, 1995, p. 986.
- [18] F. Link, H. Baumann, A. Markwitz, E.F. Krimmel, K. Bethge, *Nucl. Instrum. and Meth. B* 113 (1996) 235.
- [19] W. Möller, B.M.U. Scherzer, *Appl. Phys. Lett.* 50 (1987) 1870.
- [20] W. Möller, B.M.U. Scherzer, *J. Appl. Phys.* 64 (1988) 4860.
- [21] P. Franzen, E. Vietzke, A.A. Haasz, J.W. Davis, V. Philipps, *J. Nucl. Mater.* 196–198 (1992) 967.
- [22] P. Hammer, M.A. Baker, C. Lenardi, W. Gissler, *Thin Solid Films* 290&291 (1996) 107.
- [23] J. Roth, in: D.E. Post, R. Behrisch (Eds.), *Physics of Plasma-wall Interactions in Controlled Fusion*, vol. 131, NATO ASI Series, Series B, Plenum, New York, 1986, p. 389.
- [24] J. Roth, C. Garcia-Rosales, *Nucl. Fusion* 36 (1996) 1647.
- [25] V.Kh. Alimov, B.M.U. Scherzer, *J. Appl. Phys.* 78 (1995) 137.